A new framework integrating reinforcement learning, a rule-based expert system, and decision tree analysis to improve building energy flexibility

Zhou, Xinlei; Du, Han; Sun, Yongjun; Ren, Haoshan; Cui, Ping; Ma, Zhenjun

Published in:
Journal of Building Engineering

Published: 15/07/2023

Published version (DOI):
10.1016/j.jobe.2023.106536

Publication details:
Zhou, X., Du, H., Sun, Y., Ren, H., Cui, P., & Ma, Z. (2023). A new framework integrating reinforcement learning, a rule-based expert system, and decision tree analysis to improve building energy flexibility. *Journal of Building Engineering*, *71*, [106536]. https://doi.org/10.1016/j.jobe.2023.106536

Journal of Building Engineering 71 (2023) 106536

Contents lists available at ScienceDirect

Journal of Building Engineering

journal homepage: www.elsevier.com/locate/jobe

A new framework integrating reinforcement learning, a rule-based expert system, and decision tree analysis to improve building energy flexibility

Xinlei Zhou [a], Han Du [a], Yongjun Sun [b], Haoshan Ren [b], Ping Cui [c], Zhenjun Ma [a,*]

[a] Sustainable Buildings Research Centre, University of Wollongong, 2522, Australia
[b] Division of Building Science and Technology, City University of Hong Kong, Hong Kong
[c] School of Thermal Engineering, Shandong Jianzhu University, Jinan, 250101, Shandong, China

ARTICLE INFO

Keywords:
Reinforcement learning
Rule-based expert system
Building energy flexibility
Net-zero energy building

ABSTRACT

This study presents a new framework that integrates machine learning and a domain knowledge-based expert system to improve building energy flexibility. In this framework, a rule-based expert system was used to maximize the self-consumption of solar photovoltaics (PV) power, while a reinforcement learning (RL) agent was constructed to efficiently optimize the grid power import for battery charging and facilitate decision-making for battery discharging in response to the time of use electricity prices. Meanwhile, a Classification and Regression Tree (CART) model was developed to quantitatively analyze the relationships between building energy flexibility and external variables of interest to enhance the explainability of the framework. This work integrates the advantages of safety and simpleness of the domain knowledge-based expert system and the exploration and optimization capability of RL into building energy management. The performance of the proposed framework was evaluated using the four-year data collected from a real net zero energy office building. The system cost reduction ratio, self-consumption ratio, and self-sufficiency ratio were used as the energy flexibility indicators. The results showed that the integration of the RL and the rule-based expert system was able to reduce the electricity cost and grid power consumption by 7.0% and 10.6% respectively, and increase the self-consumption of PV power by 9.2% as compared with the use of the rule-based expert system only. The CART analysis also showed that external conditions can significantly influence the level of building energy flexibility. For instance, the average daily cost reduction ratio was 0.89 out of 1.0 when the daily maximum solar irradiance was above 717.5 W/m^2, while it decreased to 0.28 when the daily mean solar irradiance was below 62.4 W/m^2. This strategy can be used to facilitate building demand-side management and improve the design and control of building energy systems for enhanced demand flexibility.

Nomenclature

a	action
C	electricity cost

* Corresponding author.
E-mail address: zhenjun@uow.edu.au (Z. Ma).

https://doi.org/10.1016/j.jobe.2023.106536
Received 16 August 2022; Received in revised form 5 April 2023; Accepted 10 April 2023
Available online 11 April 2023

CART	Classification and Regression Tree
CRR	cost reduction ratio
DDPG	deep deterministic policy gradient
DQN	deep Q-network
HVAC	Heating Ventilation and Air Conditioning
I_{max}	daily maximum solar irradiance
I_{min}	daily minimum solar irradiance
KPI	key performance indicator
MPC	model predictive control
n	batch size of data sampling from a memory buffer
N	total number of time steps
NZE	net-zero energy
PV	photovoltaics
P_{PV}	power generation of solar photovoltaics
P_{demand}	building electricity demand
$P_{grid\text{-}building}$	grid power directly supplied to the building
$P_{grid\text{-}battery}$	grid power used to charge the battery
P_{grid}	electricity import from the grid
Q	critic network
Q'	target critic network
r	reward
RL	reinforcement learning
s	state
SCR	self-consumption ratio
SSR	self-sufficiency ratio
TOU	time of use
T_{min}	daily minimum temperature
T_{max}	daily maximum temperature
T_{mean}	daily average temperature
μ	actor network
μ'	target actor network
θ	tunable parameters of network
γ	factor discounting future rewards
δ	temporal difference error
Δt	duration of a time step

1. Introduction

Due to the rapid growth of energy consumption and the depletion of fossil fuels, the deployment of renewable energy sources in buildings is increasing worldwide in order to achieve net-zero emissions. However, it is quite challenging to match energy generation from intermittent renewable energy resources with the power demand of buildings [1]. In this context, building energy flexibility, which can assist in managing the demand and generation of buildings according to climate conditions, user needs, and grid requirements, has been proposed as an effective approach to addressing this challenge [2]. The increasing complexity of building energy systems and strong dynamics in building operations pose both challenges and opportunities in the development of energy flexibility plans in buildings.

Energy flexibility indicators, which can provide insights into building energy flexibility potential, are a significant component in the development of building energy flexibility plans. A range of energy flexibility indicators such as cost saving potential, energy saving potential, load shifting efficiency, and peak shaving efficiency have been frequently used to evaluate and quantify the energy flexibility potential of various energy flexible sources in buildings. For example, Wang et al. [3] reported that shutting down some of the chillers in a commercial building during short time demand response events can reduce energy costs by 15.3% and achieve a fast power reduction of 39%. Sánchez et al. [4] evaluated the flexibility potential of Heating, Ventilation and Air Conditioning (HVAC) systems of five residential buildings by using building thermal mass as a flexible measure. It was found that energy savings of 18.1–26.1% can be achieved by optimizing the parameter settings for preheating, precooling and night ventilation according to the operating conditions and electricity tariffs. In Ref. [5], an intelligent home energy management strategy was proposed, in which battery charging and discharging were scheduled and the temperature setpoint of the HVAC system was adjusted according to the time of use (TOU) electricity prices. It was reported that this strategy can achieve electricity cost savings by up to 20% in a residential house. The results from Ref. [6] showed that through rescheduling the operation of adjustable appliances of a residential site based on the variation in electricity prices, the cost and peak-to-average ratio of the electricity consumption were reduced by 25% and 63%, respectively.

Apart from energy flexibility indicators, control strategies are another important element to optimize building operations via appropriately using energy flexibility offered by energy flexible systems. The most conventional strategy used in buildings is a rule-based expert system, which usually relies on a set of pre-determined rules in the form of conditional statements to map control signals with system states based on expert knowledge [7]. A rule-based expert system was often used to improve the energy flexibility of building HVAC systems. For instance, a higher supply air temperature can be applied to charge building thermal mass when the electricity price is low, and the thermal mass can release the stored thermal energy to the end-users during high electricity price periods in heating seasons. The use of such a rule-based expert system can reduce the energy consumption of a low-energy apartment by up to 87% during morning peak hours [8]. A similar strategy with a lower supply air temperature can be implemented in cooling seasons. It was reported that the peak cooling energy can be reduced by 54.0% when using this strategy for indoor temperature setpoint control of a net-zero energy office building [9].

The foregoing studies have demonstrated that although the rule-based expert systems were simple enough, they were effective to improve building energy flexibility. However, the performance of rule-based expert systems is often not optimal, especially when used in complex control environments as the predictive information of future operating conditions was not leveraged in the decision-making. To solve this problem, model predictive control (MPC) was proposed [10]. In the MPC method, a model that can predict future system dynamics according to current states and future disturbances should be first developed. Based on the prediction model, the control strategy can provide the system with optimal future performance. MPC has been widely used to optimize the temperature control of building HVAC systems [11–13]. However, this method significantly relies on the prediction models used as different models offer different levels of prediction accuracy. The development of accurate yet computationally efficient prediction models often requires excellent domain knowledge and a good understanding of system details and dynamics. In addition, the performance of the prediction models may be degraded if the building operating patterns are different from the data used for model calibration.

Reinforcement learning (RL), which is a branch of machine learning, has recently gained fast development in areas such as gaming [14] and robotics [15] due to its superiority in solving sequential decision-making problems. Through interaction with the environment, an RL agent could fully utilize the exploration data and provide better control decisions without the need to develop and calibrate a model. Recently, some studies also extended the application of RL to enhance building energy efficiency and energy flexibility, and its performance was compared with conventional control methods. For example, Odonkor and Lewis [16] developed an RL controller to optimize the energy dispatch policy for a shared battery system within a building cluster. Using the historical demand profiles of different buildings as the training data, the RL controller learned an energy distribution policy for cost reduction and peak demand reduction. Jiang et al. [17] compared the performance of an RL controller with that of a rule-based expert system. A deep Q-network (DQN) model was developed to minimize the energy cost of an HVAC system based on the TOU electricity prices. Through a five-year simulation of a single-zone building model, it was found that the DQN model reduced the total cost by up to 8% when compared with a rule-based expert system. Du et al. [18] compared different RL controllers in terms of their performance in energy cost savings of a residential HVAC system. A deep deterministic policy gradient (DDPG) controller and a DQN controller were respectively implemented in a simulation environment to learn optimal control policies. The simulation results showed that the DDPG controller can achieve a reduction of 15% in energy costs and a reduction of 79% in comfort violations during a heating season, as compared with the use of the DQN controller. When compared with a rule-based expert system, the comfort violation can be reduced by 98%. Azuatalam et al. [19] proposed an efficient RL controller to optimize the operation of an HVAC system to improve energy efficiency and achieve demand response targets. It was reported that the RL controller without using demand response strategies can reduce the weekly energy consumption by 22% when compared with a default EnergyPlus HVAC controller. Furthermore, the average weekly power reduction or increase of up to 50% in different scenarios can be achieved by employing the RL controller that used demand response strategies, as compared with the one without using the demand response strategies.

The above studies demonstrated the effectiveness of using RL to enhance building energy performance. Since the RL agents rely on significant explorations in the control environment to optimize decision-making policies, the training process of these methods is both time-consuming and data demanding. In addition, the safety and robustness of RL controllers need to be improved to make sure that they will not mess up building operations, especially when sufficient data is not available for training a completely safe RL controller. Furthermore, the previous studies on building energy flexibility were only able to determine how much flexibility can be offered by implementing a flexibility measure for a certain period of time, while they did not provide insights into the interaction between building energy flexibility and external variables. Weather conditions and day of the week (i.e. Monday through Sunday) have been considered as significant factors influencing building energy usage [20,21], while their impacts on building energy flexibility potential have not been investigated in the majority of existing studies. Machine learning has been effectively used to discover relationships between the performance of building energy systems such as HVAC systems and their operating parameters [22,23]. These methods have great potential but have not yet been used in building energy flexibility evaluation.

In this study, a new framework that combines RL, a rule-based expert system, and a decision tree model was developed to improve the energy flexibility of buildings with integrated PV and battery storage systems. In this framework, a new strategy using RL and a rule-based expert system was first developed to improve building energy flexibility by using the exploration and optimization capability of RL and the control stability and robustness yet simpleness of rule-based expert systems. In this strategy, RL was used to determine the battery charging using grid power or battery discharging when the TOU electricity prices tend to increase in the next time step. The rule-based expert system was used to maximize the self-consumption of PV power. To enhance the transparency and explainability of the proposed RL-RBES strategy, a classification and regression tree (CART) model was used as a predictive model to identify the relationship between building energy flexibility and external conditions, providing insights into how the building responds to the changes to the operating conditions when using the proposed RL-RBES strategy. This information is particularly valuable for stakeholders to understand and trust the decisions made by the strategy, and it may assist in further optimization of building

performance. The novelties of this study include: (1) the first time RL was integrated with a rule-based expert system to provide a reliable and efficient approach to improving and evaluating building energy flexibility and; (2) using the CART model to examine the interactions between building energy flexibility and external variables such as weather and day of the week to enhance the explainability of the framework and provide more useful information for further improving and optimizing building energy flexibility. The performance of this framework was evaluated using the four-year data collected from a net-zero energy office building that featured solar PV panels and a battery storage system.

2. Development of the framework for improving building energy flexibility

2.1. Outline of the new framework

Fig. 1 outlines the new framework, which mainly consists of four essential components, i.e. building information collection and data preparation, development of an RL and a rule-based expert system (RL-RBES) integrated strategy for energy flexibility enhancement and evaluation, using a CART model for predictive modeling of building energy flexibility, and performance testing and evaluation of the proposed framework. In the first step, building information that influences the energy flexibility potential should be identified and collected. This information includes available energy flexible measures (i.e. PV and battery in this study), electricity tariff, constraint factors (e.g. battery storage capacity), uncertainty factors (e.g. occupancy), and other factors of interest. Other related data such as time series building demand data, PV generation data, weather data and day of the week should also be collected. These data will then be split into two datasets as training data and test data, and respectively used for RL training and testing the performance of the framework. In the second step, a rule-based expert system was first developed to determine the schedule of PV power dispatching, battery discharging, and grid power import to meet building demand when electricity price remains unchanged or decreases in the next time step. An RL agent was then constructed and integrated into the rule-based expert system to facilitate the battery charging by using grid power and battery discharging when the electricity prices tend to rise in the next time step. The RL agent was trained using the training data. In the third step, a CART model was developed for the predictive modeling of energy flexibility and investigating the interactions between building energy flexibility and external variables of interest. In the last step, the effectiveness of the RL-RBES integrated strategy was tested based on the test data. It is noteworthy that the RL agent trained in the second step will not be continuously updated using the latest data during the performance test period. Furthermore, the level of building energy flexibility was evaluated by comparing the performance achieved by using the RL-RBES integrated strategy with that of the baseline scenario in which no flexible measures were used, and the relationship between the energy flexibility potential and external variables was

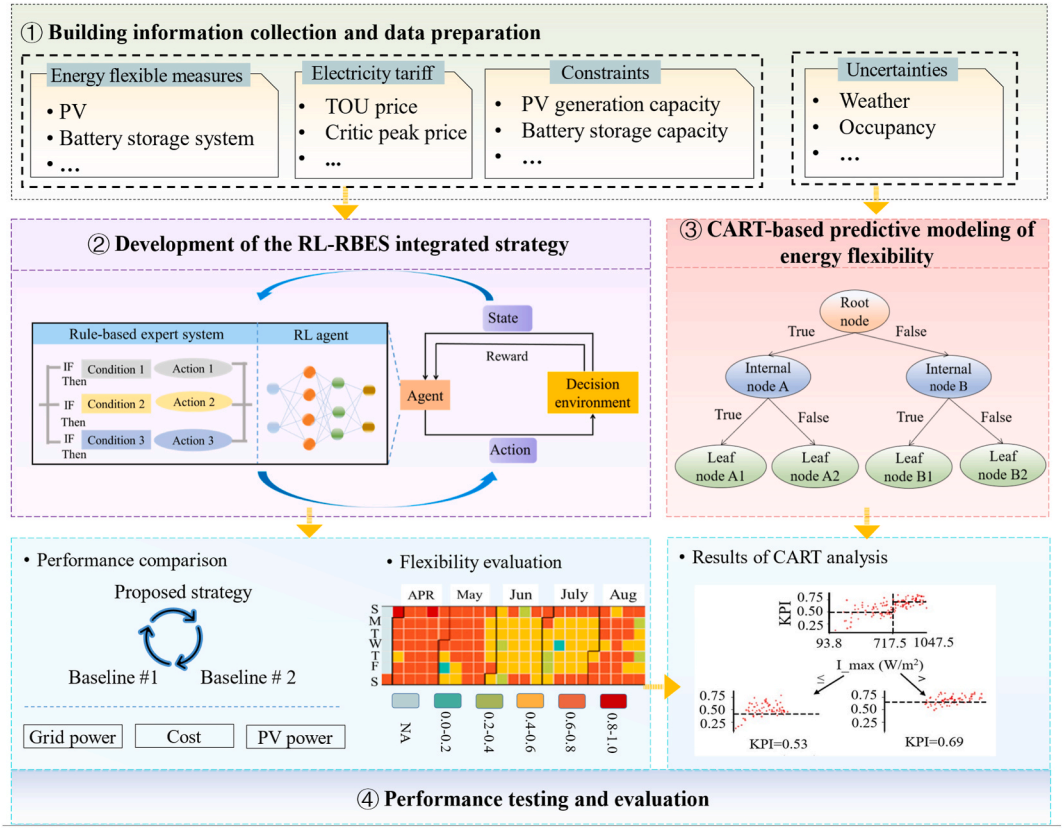

Fig. 1. Outline of the proposed framework.

examined by the CART model. The results were then visualized for further analysis to identify useful information for system design and optimization.

2.2. Development of the RL-RBES integrated strategy for energy flexibility enhancement

2.2.1. RL description

An RL algorithm is to enable an agent to interact with the decision environment and optimize its decision-making policy based on the environment exploration data [24]. There are generally two types of RL algorithms, i.e. value-based algorithms such as Q learning, Sarsa, DQN which focus on dealing with discrete actions, and policy gradient-based algorithms such as deep deterministic policy gradient (DDPG) which optimize continuous actions [25]. As the action space used to determine the battery charging and discharging is continuous, the DDPG model was therefore used in this study. The structure and working principle of the DDPG are shown in Fig. 2 c). Firstly, the agent observes an initial state (s_t), and the actor-network denoted as $\mu(s|\theta^{\mu})$ will generate a decision (a_t) according to s_t. As the agent implements the decision in the control environment, it steps to the next state (s_{t+1}) and meanwhile receives a reward (r_{t+1}). The state-action pairs (s_t, a_t) can be evaluated by using a critic network, i.e. $Q(s, a|\theta^{Q})$. The target actor-network ($\mu'(s|\theta^{\mu'})$) will generate an action (a_{t+1}) after observing the state s_{t+1}. A target critic network, i.e. $Q'(s, a|\theta^{Q'})$, is then used to evaluate the state-action pairs (s_t, a_t). The temporal difference error resulting from the $Q(s, a|\theta^{Q})$ and $Q'(s, a|\theta^{Q'})$ can be calculated by Eq. (1), where δ indicates the temporal difference error and γ donates the factor that discounts the future rewards [26].

$$\delta = r_{t+1} + \gamma Q'\left(s_{t+1}, a_{t+1}\middle|\theta^{Q'}\right) - Q\left(s_t, a_t\middle|\theta^{Q}\right) \tag{1}$$

As the agent repeats the above process, the generated experience data can be collected within a memory buffer. Based on the experience data, the temporal difference error can be minimized by adjusting the weights of the critic network, and the updated critic network can guide the updates of the actor network by using Eq. (2) to generate the optimal actions according to its observations.

$$\nabla_{\theta^{\mu}} J \approx \frac{1}{n}\sum_{i} \nabla_a Q\left(s, a\middle|\theta^{Q}\right)|_{s=s_i, a=\mu(s_i)} \nabla_{\theta^{\mu}} \mu\left(s_i\middle|\theta^{\mu}\right)|_{s_i} \tag{2}$$

where n represents the batch size of data sampling from the buffer [26].

2.2.2. Development and integration of the rule-based expert system with the RL agent

Maximizing the consumption of PV power in buildings has been applied as a common solution to reduce the peak demand for grid power and decrease the electricity costs of buildings. In this study, PV power was prioritized to be consumed by the building when PV generation is available. In this manner, a rule-based expert system was used to determine how to use PV power (i.e. supplying PV

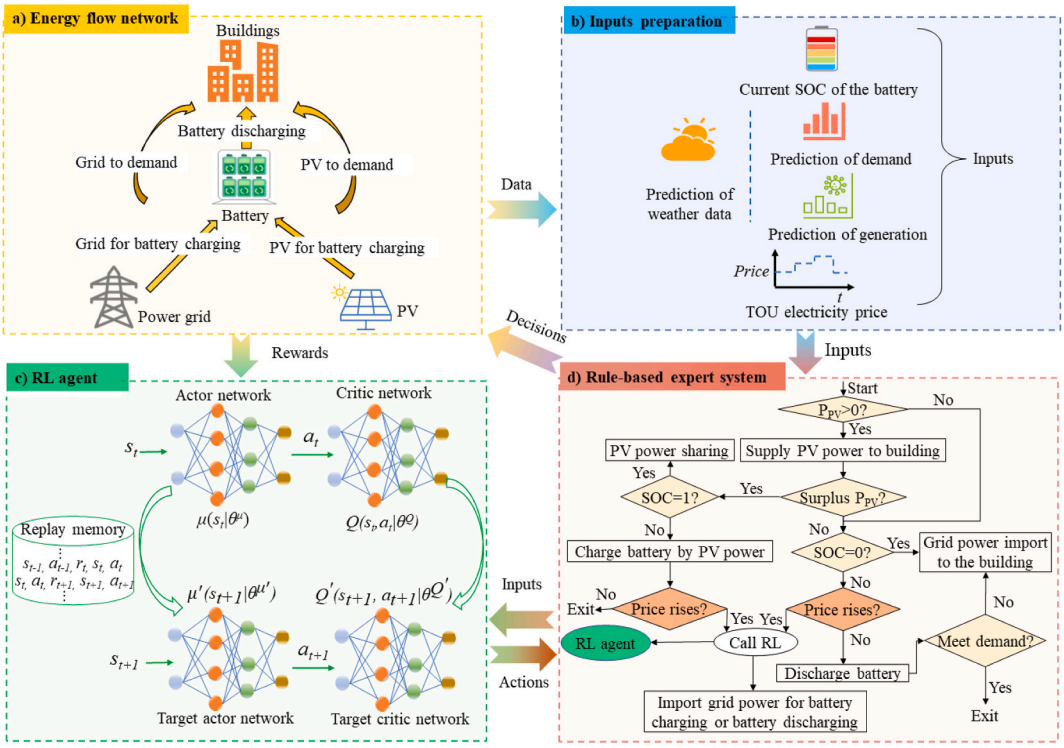

Fig. 2. Outline of the strategy using RL and a rule-based expert system.

power to meet building demand, using PV power to charge the battery, and sharing PV power with neighborhood buildings). It is noteworthy that in this study, instead of exporting surplus PV power to the grid, extra PV power was shared with the neighborhood buildings. The rule-based expert system used is described as follows.

1) PV power will be supplied to meet building demand when PV generation is available, and surplus PV power will also be used to charge the battery. Extra PV power will be supplied to the neighborhood buildings once the battery is fully charged.
2) The battery will be discharged and supplied to the building if PV power cannot meet the demand. Grid power will be imported if the battery is fully discharged. It is noted that in this analysis, the constraints for battery charging and discharging rates were not considered.

In general, the above rules are reliable when PV power and the battery can meet the electricity demand of the building. However, if PV power and the battery cannot meet building demand, grid power should be imported to provide additional power to cover the demand. Due to the variation in the electricity price of the power grid, there are opportunities to further improve building operational performance by using energy flexibility offered by the battery such as charging the battery using the grid power at a low price period and discharging the battery during the high electricity price periods. However, the above rule-based expert system cannot determine when and how much grid power should be imported to charge the battery. If the battery is always fully charged during the low electricity period using the grid power, surplus PV power cannot be used to charge the battery and thereby will result in reduced self-consumption of PV power. In addition, the above rule-based expert system discharges the battery whenever the building demand cannot be covered by the PV power. However, if the PV power and battery were not able to cover the electricity demand, the battery power is preferred to be discharged during peak hours instead of off-peak hours to reduce the electricity cost. To solve these problems, RL was integrated with the rule-based expert system to develop a more robust strategy that can facilitate the decision-making in battery charging and discharging to reduce the electricity cost without sacrificing the self-consumption of PV power.

The detailed strategy is illustrated in Fig. 2. Firstly, the state of charge (SOC) of the battery at the current time step and the TOU electricity price data should be collected, and the hourly data of PV generation, electricity demand for the next 24 h should be predicted based on the prediction of the weather data. It is noteworthy that in this study, the analysis was based on the four-year historical data, and therefore the prediction models of the PV generation and electricity demand were not considered and perfect predictions in these data were assumed. These data were formulated as the input data and supplied to the rule-based expert system. If the electricity tariff was predicted not to increase in the next time step, the rule-based expert system was then used to determine the schedule of PV power dispatching, battery discharging and grid power import. If the electricity tariff was predicted to increase in the next time step, the strategy will then integrate the RL into the rule-based expert system, and the RL will be used to determine how much grid power should be imported to charge the battery or how much power should be discharged from the battery when PV power cannot cover the demand. It is noteworthy that the battery charging and discharging cannot occur simultaneously. In this study, the RL instant reward was the cost reduced by using the RL-RBES integrated strategy compared with the scenario that used a rule-based expert system only. The daily total cost reduction was the total reward for the RL agent during its training process. As the training process iterates, the RL agent can learn an optimal policy to determine battery charging and discharging when there is an increase in the electricity price in the next time step.

2.3. CART model for predictive modeling of building energy flexibility

CART is a widely used decision tree algorithm that can be either used in prediction tasks when the data concerned is numeric or in classification tasks when the data of interest is categorical [27]. In both tasks, the CART model can classify the target variable into several groups according to explanatory variables using a recursive binary data splitting method [28]. In this study, a CART model was developed to quantitatively analyze the building energy flexibility potential under the impact of different external conditions. The weather data (i.e. daily maximum and mean solar irradiances, and daily maximum, mean and minimum outdoor temperatures) and the

Fig. 3. Illustration of the case study building.

day of the week were considered as the explanatory variables and the building energy flexibility data were used as target variables to train the CART model. Once the model was trained, it was then visualized to demonstrate the relationship between external variables and building energy flexibility.

3. Performance testing of the proposed framework

3.1. Description of the case study building and data used for analysis

The case building used for testing the performance of the proposed framework is a net-zero energy office building at the University of Wollongong, Australia. The building consists of two interconnected wings with a total floor area of 2600 m^2, as shown in Fig. 3. The southern wing has two stories. The first floor is an open-plan office and the ground floor consists of an exhibition space, laboratories, teaching spaces, and amenities. The northern wing is a high bay workshop space, which is naturally ventilated. To reduce building energy consumption, a wide range of renewable and energy-efficient systems were used in this building such as PV panels, transpired solar collectors, a ground source heat pump system, an air source heat pump system, a battery storage system, and cool roofs. As the main power generation source, PV arrays with a generation capacity of 160 kW, and a battery with a storage capacity of 39.6 kWh were selected as the flexible sources in this study although the HVAC system also offers some degrees of energy flexibility. The main electricity consumers of the building include the HVAC system, lighting, computers, lifting, overhead crane, and plug-in equipment such as an electric car charging station and experimental facilities.

The PV generation data and the electricity demand data used in this study were from January 1, 2017 to December 31, 2020 with a resolution of 1 h, which was collected from the Building Management System. The data from 2017 to 2018 were used for the RL agent training while that from 2019 to 2020 were used for testing the performance of the RL-RBES integrated strategy and the framework developed. It is noted that missing data for a short time (i.e. within 1 h) was filled using linear interpolation, while those missing for more than 1 h were not used in this study. The PV electricity generation data and building electricity demand data in 2017 are illustrated in Fig. 4.

The daily TOU electricity price data used in this study are presented in Table 1, which was sourced from the Business Flexible Server

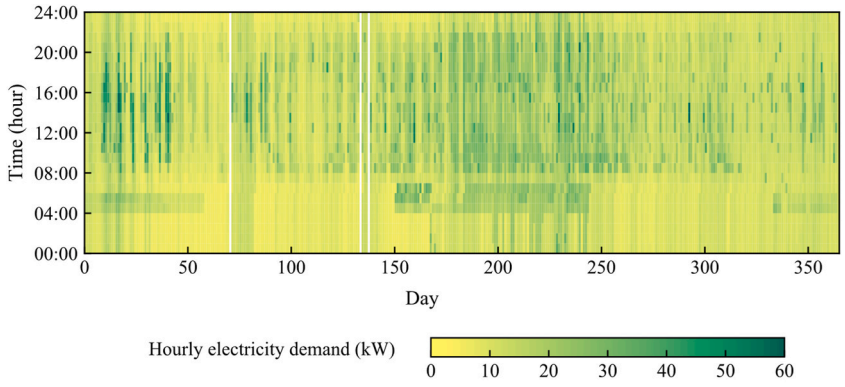

a) Hourly-based electricity demand of the case building.

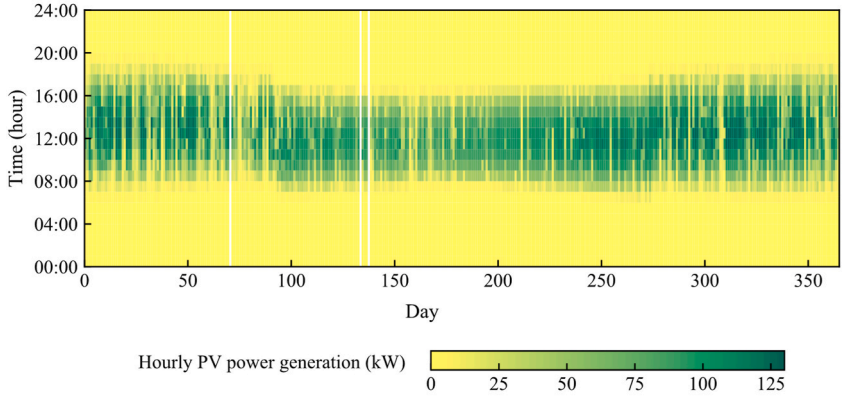

b) Hourly-based PV power generation.

Fig. 4. Hourly-based electricity demand and PV power generation of the case building.

of the Australian Gas Light Company [29].

In the CART analysis, only the weather data (including outdoor temperature and solar irradiance) and the day of the week were considered as the external variables that influence the flexibility potential of the building. Due to the sensor fault, only the weather data from July 31, 2020 to December 19, 2020 were collected from the Building Management System and were used for CART analysis in this study.

3.2. Performance evaluation of the RL-RBES integrated strategy for building energy flexibility enhancement

The performance of the RL-RBES integrated strategy was tested using the test data from January 01, 2019 to December 31, 2020. The PV generation and electricity demand profiles of several selected representative days are illustrated in Fig. 5 to demonstrate how this strategy can improve building energy flexibility by optimizing the battery charging and discharging. In this analysis, the same battery charging and discharging efficiency of 0.92 was used, according to Ref. [30].

It can be observed from Fig. 5 a)-c) that the grid power was imported to charge the battery before 7 a.m. if PV generation and the battery were not enough to cover the electricity demand of the building of that day. However, the SOC of the battery during the off-peak hours was different under different scenarios. As shown in Fig. 5 a), the RL agent did not fully charge the battery before 7 a.m. on that test day. Instead, the battery was partially charged before 7 a.m. in order to meet the demand in the following three or four hours, and after that, PV power started to be surplus and was used to charge the battery. When PV power was much less than the demand during the shoulder hours as shown in Fig. 5 b), the RL agent decided to fully charge the battery before 7 a.m. in order to shift the grid power demand from the shoulder hours to off-peak hours. If the building demand was much higher than PV generation during both peak and shoulder hours, the battery was fully charged before 7 a.m. and discharged during the shoulder hours and charged again before 1 p.m. in order to reduce grid power during the peak demand periods, as shown in Fig. 5 c). From Fig. 5 d), it can be seen that the grid power will not be used to charge the battery at all when the PV was in extreme surplus on the test day since PV power alone can fully charge the battery and cover the electricity demand of the building during peak and shoulder hours.

From Fig. 5 e), it can be seen that only a small fraction of battery power was discharged to meet the demand before 1 p.m., and grid power was imported to meet the additional demand that was not covered by PV power and discharged battery power. The majority of the battery power was discharged to reduce the grid power import during the following peak hours to decrease the electricity cost. The above results demonstrated the potential of this strategy to further improve energy flexibility by optimizing battery charging and discharging.

The amounts of electricity charged to the battery by using PV power and gird power for all the test days in 2019 and 2020 are presented in Fig. 6 a) and b), respectively. It can be observed that for the majority of the test days, PV power became to be surplus and was used to charge the battery between 7 a.m. and 9 a.m. Grid power was also frequently used to charge the battery before 7 a.m. especially when PV power became to be surplus after 9 a.m. The power charged in the battery was frequently used to reduce the grid power import during shoulder and peak hours (i.e. from 7: 00 to 22: 00) when the PV generation was not sufficient to cover the demand as shown in Fig. 6 c). It is noteworthy that in some cases, a small fraction of battery power was discharged during the off-peak hours (after 22: 00) as shown in Fig. 6c). This is because the battery power was not fully discharged during peak and shoulder hours, and the remaining battery power was then used to reduce the grid power import during the following off-peak hours. However, it was found that the battery was not always charged with grid power during the shoulder price periods as shown in Fig. 6 b). This is because the difference between the shoulder electricity price and peak electricity price was insignificant. Due to the presence of the power charging and discharging efficiencies, limited cost-saving potential can be resulted from charging the battery during shoulder hours and discharging it during peak price hours. The strategy thereby made a careful decision to charge the battery during the shoulder price periods. Another reason is that surplus PV power was usually available to charge the battery and grid power was less frequently required to charge the battery during this time period.

The performance of the RL-RBES integrated strategy was further evaluated under different scenarios presented in Table 2. Three indicators, including self-consumption ratio (SCR), self-sufficiency ratio (SSR) and cost reduction ratio (SRR), as expressed in Eqs. (3)–(5), were used to evaluate the flexibility potential achieved under different scenarios [31,32].

$$SCR = \frac{\sum_{i=1}^{N} P_{demand,i}\Delta t - \left(\sum_{i=1}^{N} P_{grid-building}\Delta t + \eta_{discharging} \cdot \eta_{charging} \cdot \sum_{i=1}^{N} P_{grid-battery,i}\Delta t\right)}{\sum_{i=1}^{N} P_{PV,i}\Delta t} \tag{3}$$

$$SSR = \frac{\sum_{i=1}^{N} P_{demand,i}\Delta t - \left(\sum_{i=1}^{N} P_{grid-building}\Delta t + \eta_{discharging} \cdot \eta_{charging} \cdot \sum_{i=1}^{N} P_{grid-battery,i}\Delta t\right)}{\sum_{i=1}^{N} P_{demand,i}\Delta t} \tag{4}$$

Table 1
Time of use electricity price used in this study.

Time	Electricity price (AUD)
00: 00–07: 00	0.1349
07: 00–13: 00	0.2936
13: 00–20: 00	0.3564
20: 00–22: 00	0.2936
22: 00–24: 00	0.1349

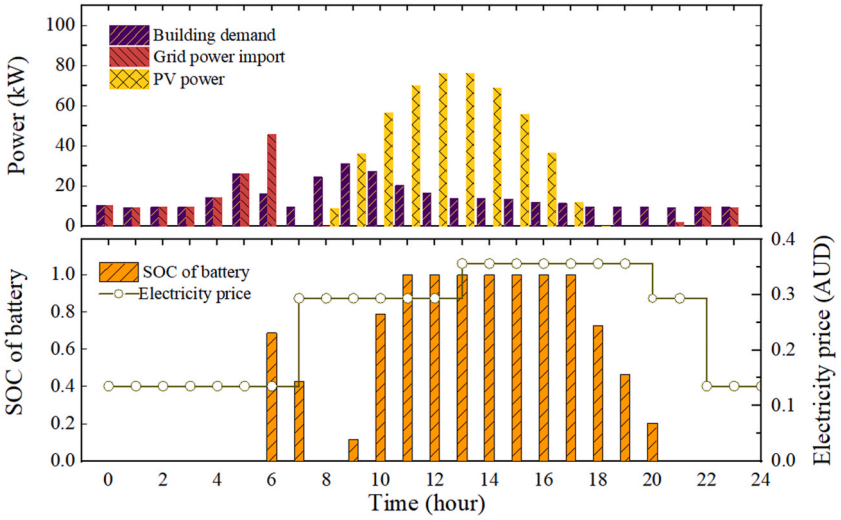

a) Battery partially charged by grid power before 7 am.

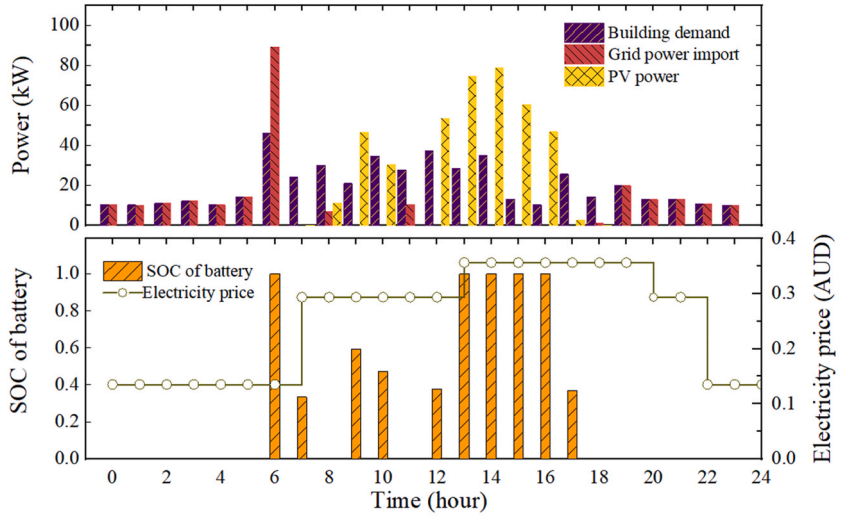

b) Battery fully charged by grid power before 7 am.

Fig. 5. Test results based on the selected representative days.

$$CRR = \frac{\sum_{i=1}^{N} C_i \bullet P_{demand,i}\Delta t - \sum_{i=1}^{N} C_i \bullet P_{grid,i}\,\Delta t}{\sum_{i=1}^{N} C_i \bullet P_{demand,i}\Delta t} \tag{5}$$

where P_{PV} is the PV power generation, P_{demand} is the building electricity demand, $P_{grid\text{-}building}$ is the grid power directly supplied to the building, $P_{grid\text{-}battery}$ is the grid power used to charge the battery, C presents the electricity cost, P_{grid} is the electricity import from the grid, N is the total number of time steps, which was 24 for a day, and Δt is the duration of a time step, i.e. 1 h in this study. $\eta_{charging}$ *and* $\eta_{discharging}$ indicate battery charging efficiency and discharging efficiency, respectively.

The baseline scenario did not use PV and the battery, and grid power was used to cover all building demand. In Scenario #1, PV was used to supply the electricity to the building and surplus PV power was shared with the neighboring buildings, while grid power was used when PV generation is insufficient.

In Scenarios #2-#4, both PV and the battery were used. Scenarios #2 and #3 both used the rule-based expert system. However, grid power was not used to charge the battery in Scenario #2, while grid power was used to fully charge the battery during the off-peak

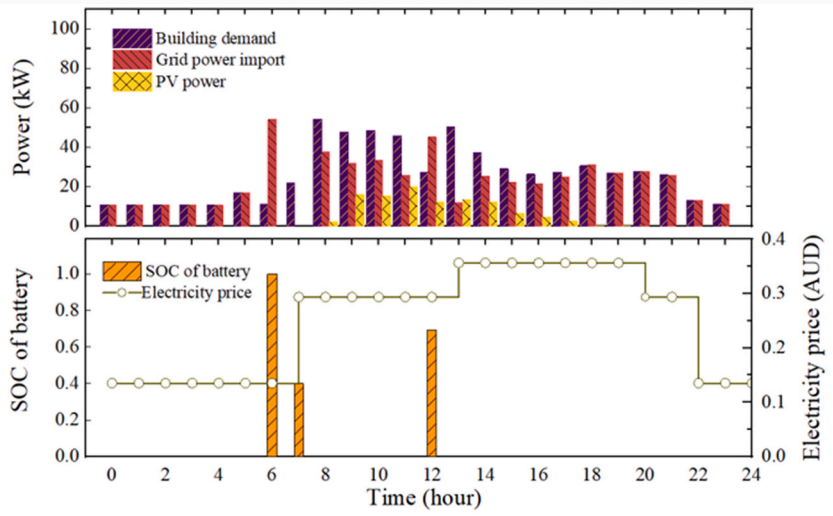

c) Battery charged by grid power before 7 am and 1 pm.

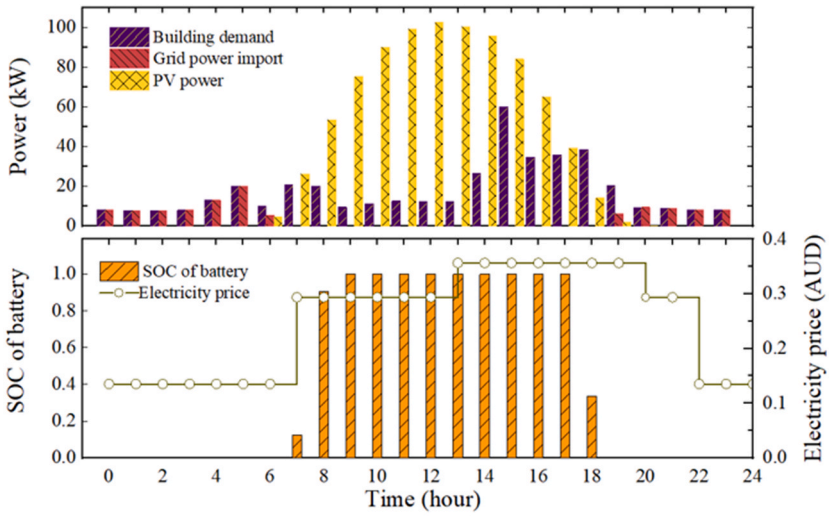

d) No battery charging by grid power.

Fig. 5. (*continued*).

period in Scenario #3. In Scenario # 4, the proposed RL-RBES integrated strategy was used.

The performance of these scenarios is compared in Fig. 7 in terms of the three energy flexibility indicators used. It is noteworthy that the values of flexibility indicators in Fig. 7 were calculated based on the daily data of the whole performance testing period according to Eqs. (3)–(5). It can be observed that Scenarios #2–4 outperformed the baseline strategy. Scenario #4 using the proposed strategy showed the overall best flexibility and achieved the lowest cost as compared with the other scenarios, although its grid power consumption and PV power consumption were similar to that of Scenario #2.

Table 3 summarizes the performance improvements of Scenario #4 which used the RL-RBES integrated strategy in comparison with Scenarios #2 and #3, which used the rule-based expert system only. It was shown that the RL-RBES integrated strategy can reduce the electricity cost by up to 4.6% and 7.0% respectively, as compared with Scenario #2 and Scenario #3. The grid power consumption was reduced by 10.6% and PV power consumption was increased by 9.2% when compared with Scenario #3. This is because, in Scenario #3, the battery was always charged by the grid power during off-peak hours to decrease grid power consumption during shoulder or peak hours. However, this practice can limit the storage capacity of the battery to store surplus PV power during peak or shoulder hours, ultimately reducing the self-consumption of PV power. The proposed strategy can properly optimize the grid power import for battery charging, ensuring that storage capacity is available for surplus PV power. It is noteworthy that the RL-RBES integrated strategy led to a slight increase in the grid power consumption due to the power loss during the battery charging and discharging, and

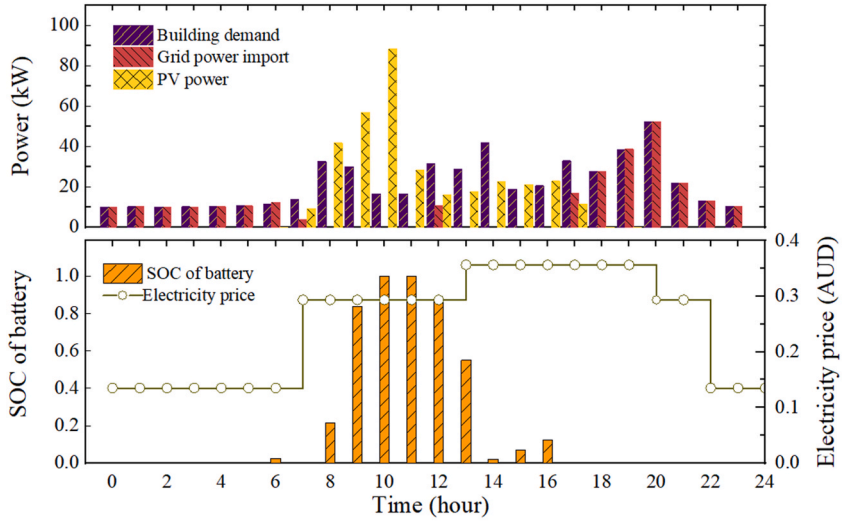

e) Battery partially discharged before 1 pm.

Fig. 5. (*continued*).

an 0.1% decrease in the PV power consumption, when compared with Scenario #2. However, these values were acceptable when considering the increase in the cost reduction ratio achieved by the RL-RBES integrated strategy.

Calendar heat maps of different flexibility indicators during the performance test periods are shown in Figs. 8–10. It can be observed that, for cost reduction ratios and self-sufficiency ratios, the days in the summer time were higher than those in the winter time due to abundant solar irradiance in summer. In terms of the self-consumption ratio, higher values were observed during winter time. The self-consumption ratio of the majority of the days was in the range of 0.4 (40%) - 1.0 (100%) during July and August of 2020. This is because solar irradiance was not abundant during this period, and a large proportion of PV power generated was consumed by the building.

3.3. Results of classification and regression tree analysis

To investigate the relationship between energy flexibility indicators and external variables, the data of the daily maximum and mean solar irradiances, daily minimum, maximum and mean outdoor temperatures, and the day of the week were extracted from the weather dataset and used as interest external variables for analysis. The importance of different variables in terms of their influences on the flexibility indicators was first identified using the CART model, and the results are shown in Fig. 11.

It can be observed that solar irradiance was the most important variable that influenced the flexibility potential of the building. The maximum solar irradiance was the most important influential variable for the cost reduction ratio and self-sufficiency ratio, while the daily mean solar irradiance was the most significant influential variable for the self-consumption ratio. According to Ref. [33], the features with the top 50% importance factors were used in the CART analysis for each flexibility indicator, and the results are shown in Figs. 12–14. In each figure, the values of the flexibility indicator were classified into several groups based on the values of explanatory variables. It can be observed that, in Figs. 12 and 13, when the daily maximum solar irradiance was above 717.5 W/m^2 and the daily mean solar irradiance was above 317.0 W/m^2, the daily average cost reduction ratio was 0.89. When the daily maximum solar irradiance was above 717.5 W/m^2, the daily mean temperature was higher than 19.5 °C and the mean solar irradiance was above 202.4 W/m^2, the daily average self-sufficiency ratio can reach 0.75. However, when the daily mean solar irradiance was below 62.4 W/m^2, the daily average cost reduction ratio and the self-sufficiency ratio were only 0.28 and 0.21, respectively.

The daily average self-consumption ratio was higher than 0.65 when the daily mean solar irradiance was less than 132.2 W/m^2 and can even reach 0.98 when the daily maximum solar irradiance was less than 331.2 W/m^2 due to the limited PV power generation (Fig. 14). However, when the daily mean solar irradiance was higher than 186.7 W/m^2, and the daily mean temperature was less than 22.3 °C, the daily average self-consumption ratio was only 0.35, due to the relatively higher PV power generation but lower building electricity demand. The information discovered by the CART analysis can be helpful to further assist in improving the energy flexibility of the case study building.

The CART analysis identified the energy flexibility level of the case study building under different external conditions. However, the conclusions generated from the CART analysis may not be able to directly apply to other buildings with different system designs or buildings located in different climate zones. Since the flexibility level of the building is closely linked with its demand, the capacities of PV generation and battery storage, the building flexibility levels under different ratios among daily maximum PV generation, daily maximum electricity demand, and battery capacity were summarized based on the results of CART analysis. These results are presented in Appendix to provide useful references for system design and performance evaluation of other buildings.

This study then investigated the impact of battery capacity on the energy flexibility level of the building. Various scenarios were

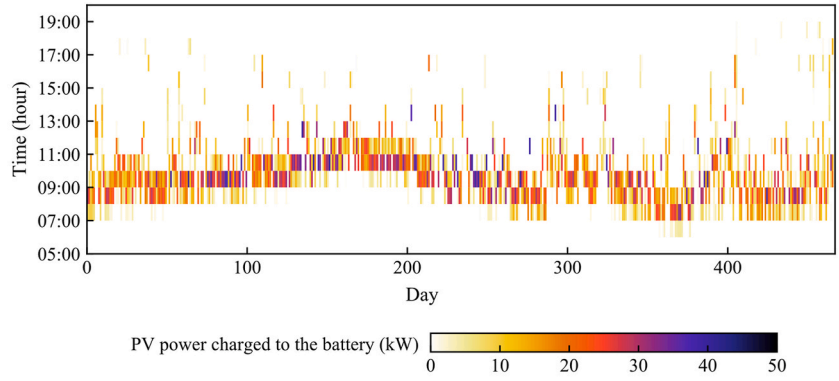

a) Battery charging by PV power.

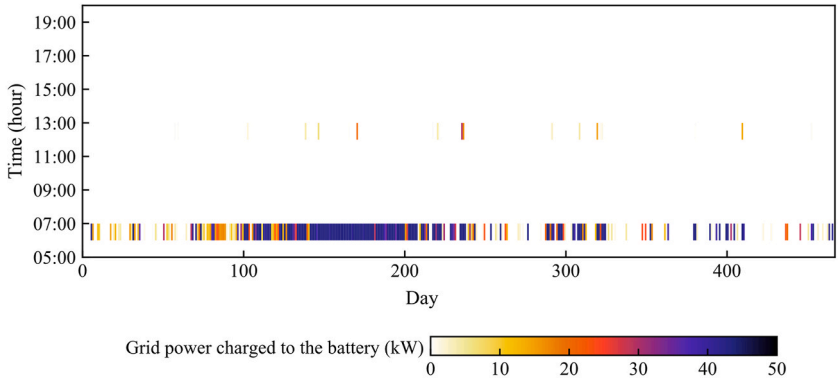

b) Battery charging by grid power.

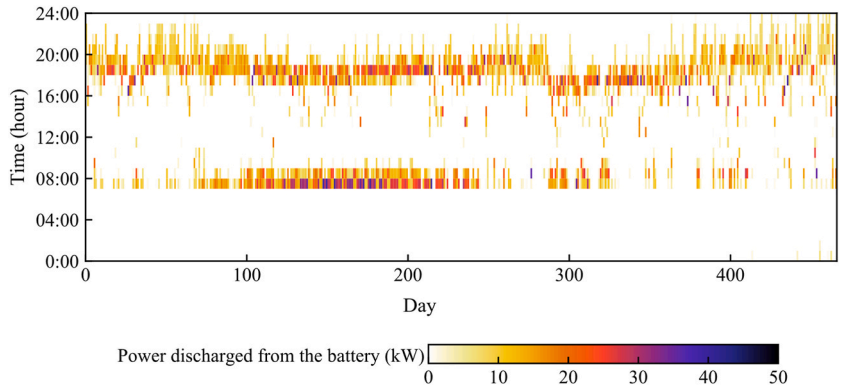

c) Battery discharging.

Fig. 6. Battery charging and discharging during the test days.

Table 2
Different scenarios designed for performance comparison.

Scenarios	PV	Battery	Considering battery charging by grid power	Rule-based expert system only	RL-RBES integrated strategy
Baseline	No	No	N/A	Yes	No
Scenario #1	Yes	No	N/A	Yes	No
Scenario #2	Yes	Yes	No	Yes	No
Scenario #3	Yes	Yes	Yes	Yes	No
Scenario #4	Yes	Yes	Yes	No	Yes

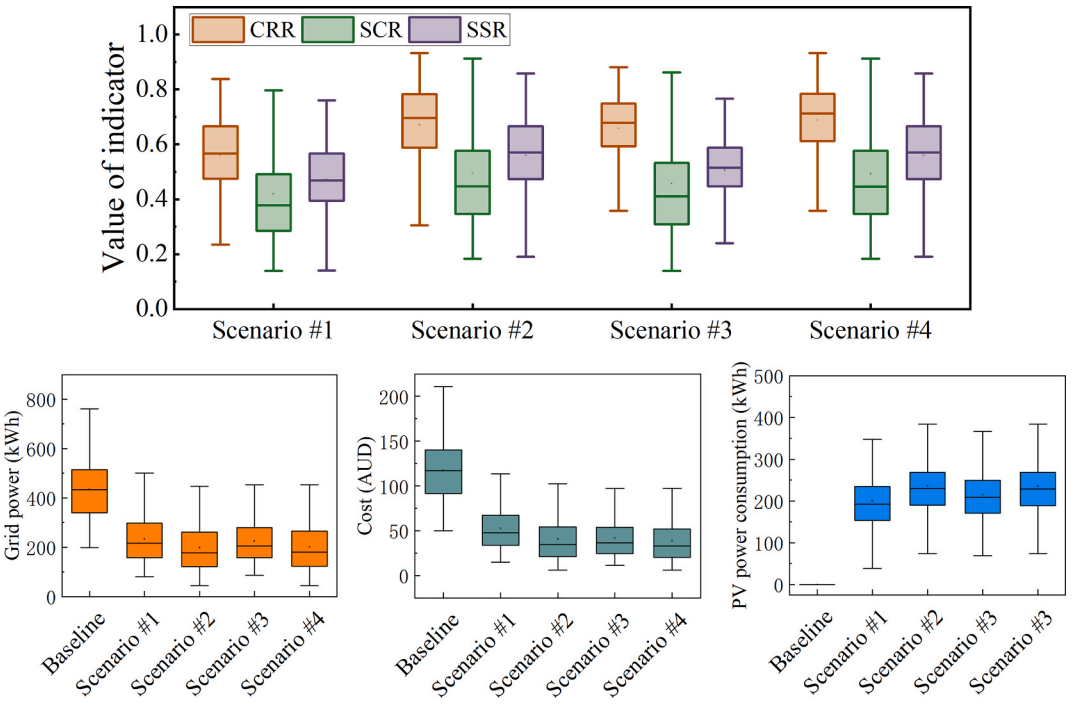

Fig. 7. Performance comparison between the scenarios using the RL-RBES integrated strategy and those using rule-based expert systems only.

Table 3
Performance improvement of using the RL-RBES integrated strategy in comparison with the rule-based strategies.

Comparisons	Cost	Grid power consumption	Consumption of PV power
Scenario #4 compared with Scenario #2	4.6%↓	1.5%↑	0.1↓
Scenario #4 compared with Scenario #3	7.0%↓	10.6%↓	9.2%↑

developed with the battery capacity ranging from 0 kWh to 81 kWh, which corresponded to 0%–60% of the maximum hourly PV generation (i.e. ~135 kWh) according to the historical data. Given the strong dynamics of PV generation and the relative stability of the building electricity demand, the building energy flexibility levels under different battery capacity design scenarios were evaluated under high solar irradiance and low solar irradiance conditions. Based on the CART analysis in Figs. 12–14, the conditions, when the daily maximum solar irradiation was above 717.5 kW/m^2, and the daily average solar irradiation was above 317 kW/m^2, were selected as high solar irradiance conditions, while the conditions, when the daily mean solar irradiance was below 62.4 kW/m^2, was considered as low solar irradiance conditions. The values of different flexibility indicators under different scenarios of battery capacity design and different external conditions are shown in Figs. 15 and 16, respectively.

The observations from Fig. 15 indicated that increasing battery capacity led to noticeable increases in all flexibility indicators when the solar irradiance was high, as the higher battery capacity enabled storage of more surplus PV power, which can be used to meet building demand when PV generation is insufficient. However, during low solar irradiance conditions as illustrated in Fig. 16, an increase in battery capacity may not considerably enhance the SCR and SSR, although there was a significant improvement in the CRR, particularly when the battery capacity exceeded 27.0 kWh. This is primarily due to the limited surplus PV generation during low solar irradiance conditions, causing the battery to primarily facilitate grid power import to reduce electricity costs, as mentioned in Section 3.2. These results can offer valuable insights into the optimization of battery capacity to maximize building energy flexibility, taking into account the impact of weather and climate conditions, as well as the cost of the battery.

4. Conclusion

This paper presented a new framework that used reinforcement learning (RL), a rule-based expert system and a Classification and Regression tree (CART) to improve building energy flexibility. In this framework, an integrated strategy employing an RL agent and a rule-based expert system (RL-RBES) was used to maximize the self-consumption of PV power and minimize the electricity cost by optimizing the grid power import for battery charging and battery discharging according to the time of use electricity prices. A CART model was used to quantify building energy flexibility under different external conditions to evaluate the building performance under changing environments and provide useful information for building design and optimization. The energy consumption data and PV power generation data from 2017 to 2020, time of use electricity prices, weather data, and day of the week information were used to

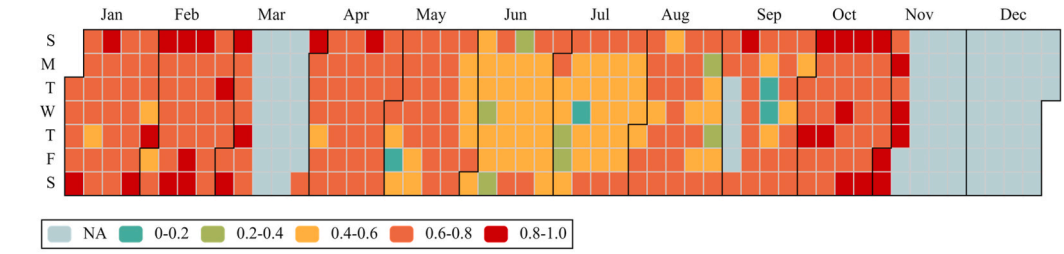

a) 2019

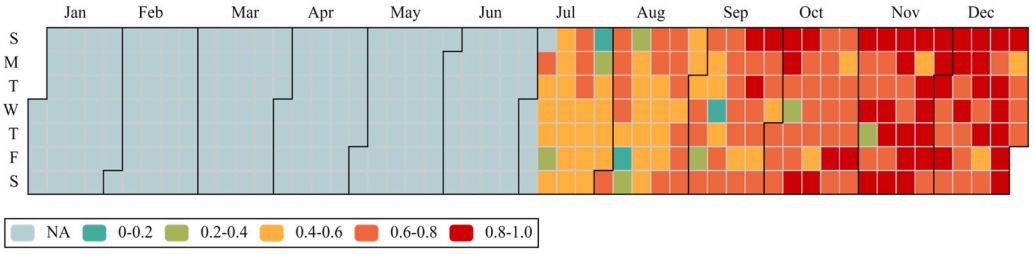

b) 2020

Fig. 8. Cost reduction ratios due to the use of the RL-RBES integrated strategy.

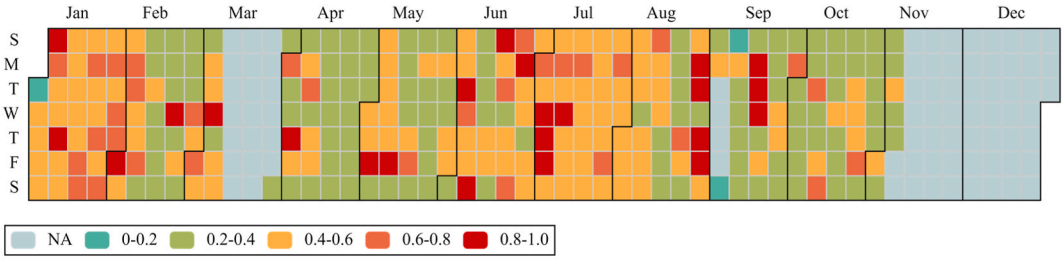

a) 2019

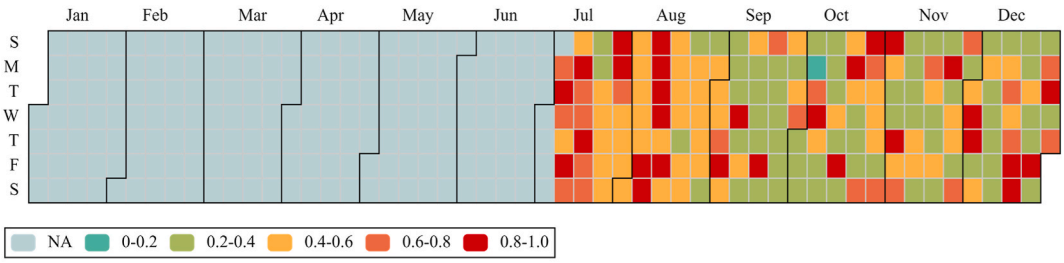

b) 2020

Fig. 9. Self-consumption ratios due to the use of the RL-RBES integrated strategy.

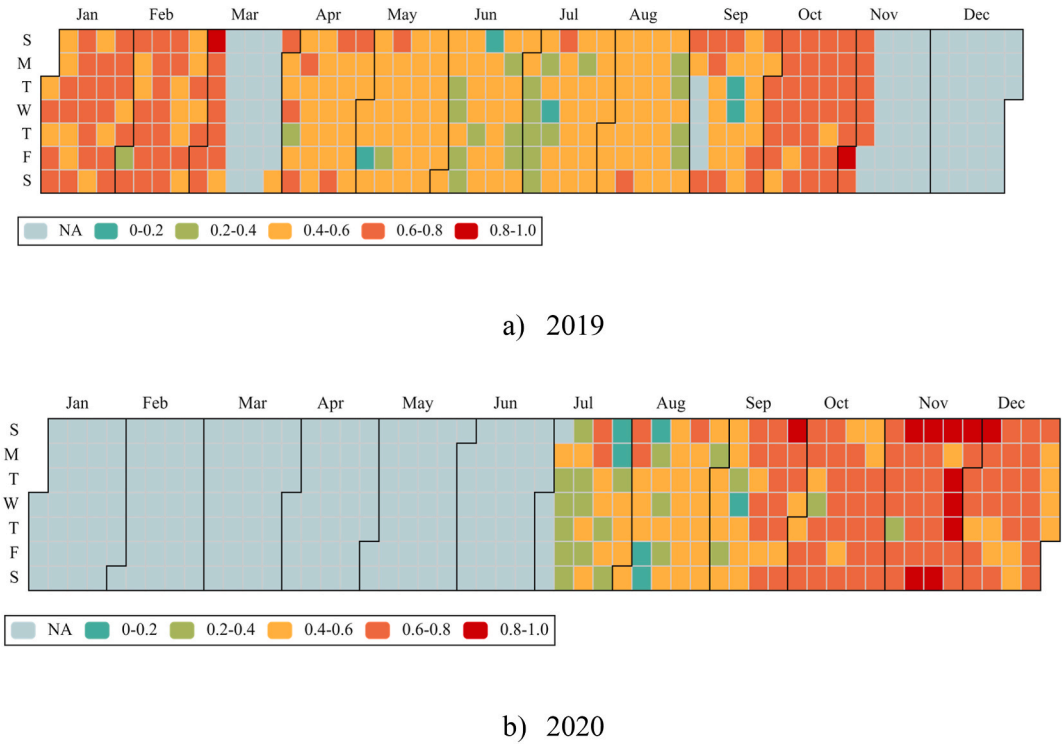

Fig. 10. Self-sufficiency ratios of the PV power due to the use of the RL-RBES integrated strategy.

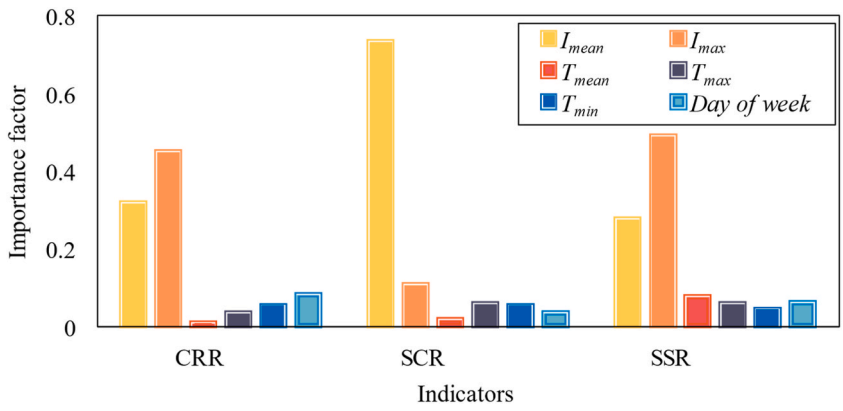

Fig. 11. Importance factors of different variables in terms of their influences on different flexibility indicators (where I_{max} and I_{mean} represent the daily maximum and mean solar irradiances, respectively; T_{min}, T_{max} and T_{mean} indicate daily minimum, maximum, and mean outdoor temperatures, respectively).

test the performance of the proposed framework. It was found that the RL-RBES strategy can reduce the two-year electricity costs of the building by 4.6% while maintaining the self-consumption of PV power and self-sufficiency at similar levels when compared with the rule-based expert system which did not charge the battery using grid power. Compared with the rule-based expert system which fully charged the battery during low electricity price periods, the proposed strategy can reduce the energy cost by up to 7.0%, and increase the self-consumption ratio and self-sufficiency ratio by up to 10.6% and 9.2%, respectively.

The CART analysis identified the daily maximum solar irradiance as the most significant variable influencing the cost reduction ratio and the self-sufficiency ratio, while the daily mean solar irradiance was the most significant factor affecting the PV power self-consumption ratio. The maximum daily cost reduction ratio, self-sufficiency ratio and self-consumption ratio of the building can reach 0.89, 0.75 and 0.98 when the RL-RBES strategy was used. Furthermore, increasing the battery size can further increase the flexibility level of the building, particularly under high solar irradiance conditions. It can also reduce the electricity cost during low solar irradiance conditions. The findings of this study can be beneficial for optimizing building operations and design.

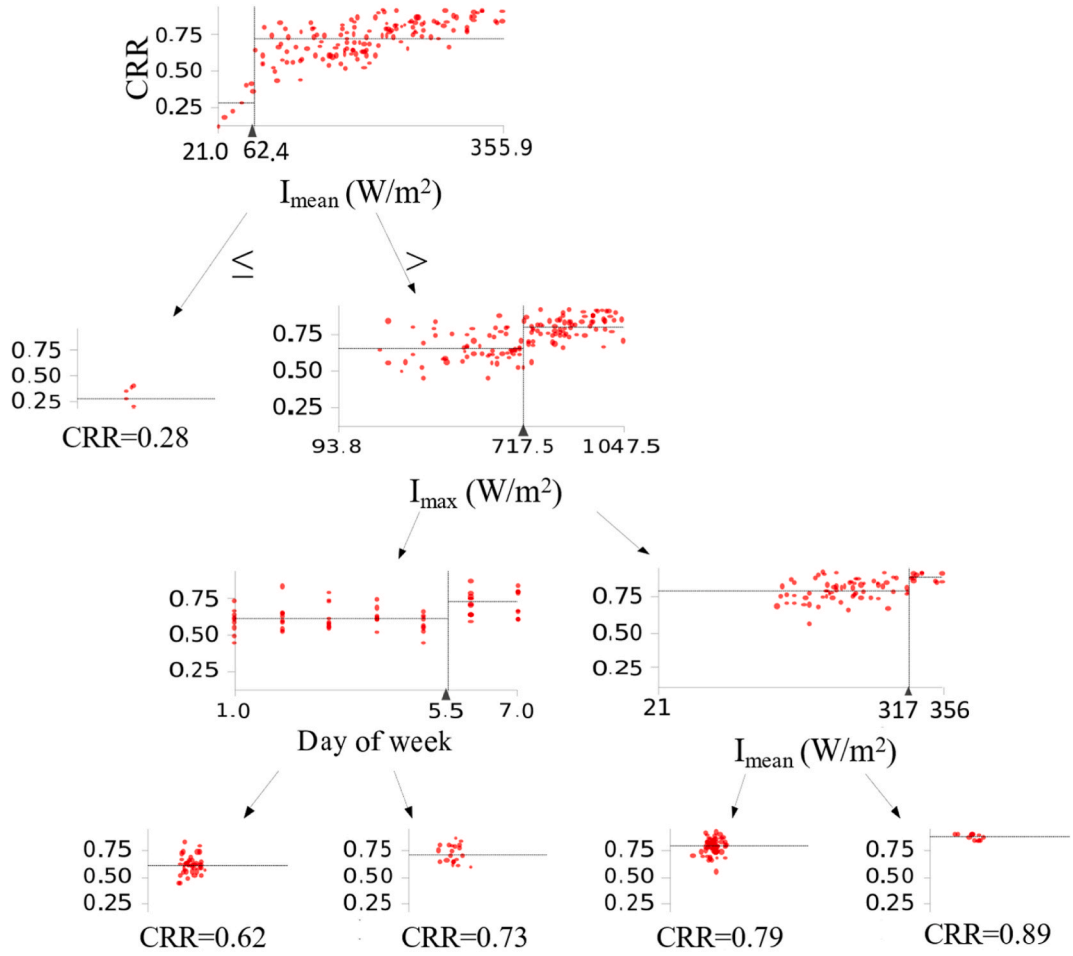

Fig. 12. Relationships between the external variables and the cost reduction ratio.

Credit author statement

Xinlei Zhou: Methodology, data analytics, and original draft preparation; **Han Du**: Visualization; **Yongjun Sun**: Reviewing and editing; **Haoshan Ren**: Reviewing and editing; **Ping Cui**: Reviewing and editing; **Zhenjun Ma**: Supervision, methodology, reviewing and editing.

Declaration of competing interest

The authors declare that they have no known competing financial interests or personal relationships that could have appeared to influence the work reported in this paper.

Data availability

Data will be made available on request.

Appendix

Table I presents the impact of the ratios among daily maximum PV generation, daily maximum electricity demand, and battery capacity on the energy flexibility levels based on the data grouped by the CART analysis in Figs. 13–15. The results showed that a larger ratio between daily maximum PV generation and battery capacity increased the CRR and SSR but decreased the SCR, as battery capacity limited PV power consumption. While variations in generation and demand profiles introduced some uncertainties, this information remained valuable for system design and can be used as a reference to evaluate buildings with different system designs.

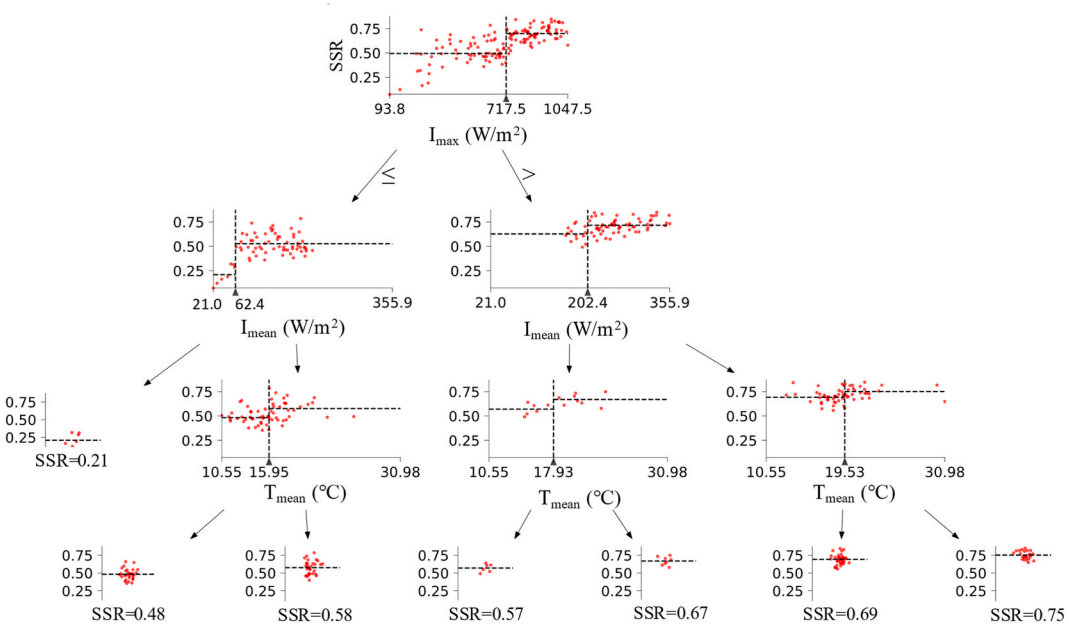

Fig. 13. Relationships between the external variables and the self-sufficiency ratio.

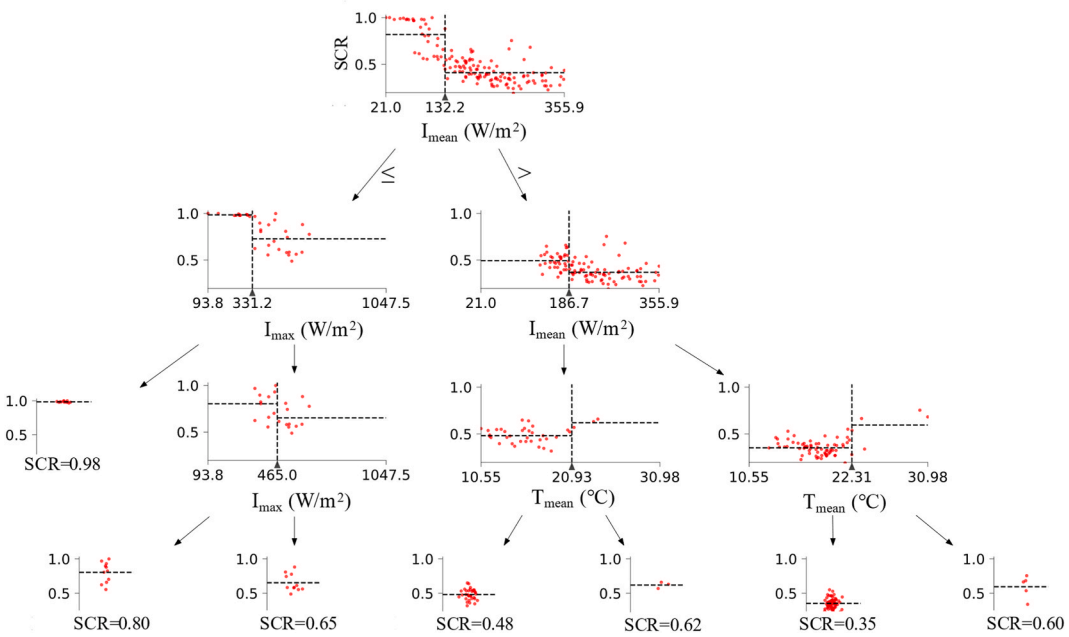

Fig. 14. Relationships between the external variables and the self-consumption ratio.

Table I
Energy flexibility indicators under different ratios among PV power, electricity demand and battery capacity.

Groups	P_{max}: D_{max}: C_b	P_{ave}: D_{ave}: C_b	CRR	SCR	SSR
Fig. 13	2.59 : 0.87 : 1	0.87 : 0.37 : 1	0.89	0.33	0.78
	2.44 : 0.68 : 1	0.68 : 0.39 : 1	0.79	0.40	0.69
	1.74 : 0.41 : 1	0.41 : 0.36 : 1	0.73	0.58	0.59
	1.84 : 0.46 : 1	0.46 : 0.53 : 1	0.62	0.61	0.50

(*continued on next page*)

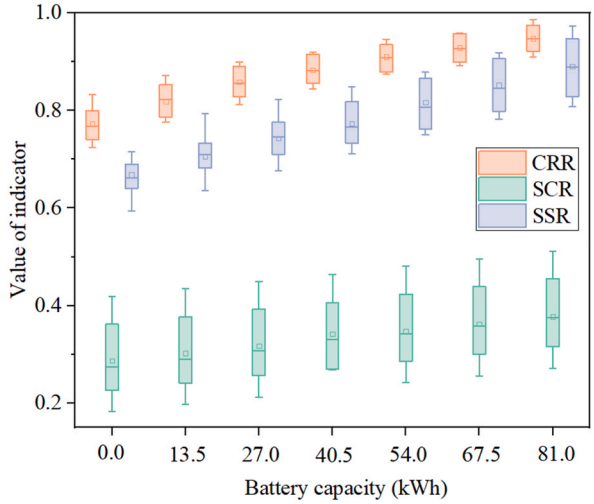

Fig. 15. Energy flexibility levels of different scenarios of battery capacity design under high solar irradiance conditions.

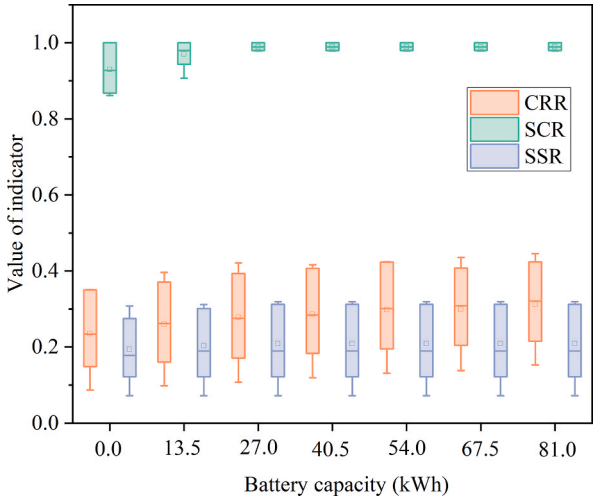

Fig. 16. Energy flexibility levels of different scenarios of battery capacity design under low solar irradiance conditions.

Table I (*continued*)

Groups	P_{max}: D_{max}: C_b	P_{ave}: D_{ave}: C_b	CRR	SCR	SSR
	0.70 : 0.11 : 1	0.11 : 0.55 : 1	0.28	0.99	0.21
Fig. 14	2.49 : 0.76 : 1	0.76 : 0.40 : 1	0.85	0.40	0.75
	2.53 : 0.75 : 1	0.75 : 0.36 : 1	0.80	0.98	0.69
	2.14 : 0.50 : 1	0.50 : 0.38 : 1	0.78	0.98	0.67
	2.40 : 0.58 : 1	0.58 : 0.46 : 1	0.69	0.98	0.57
	1.59 : 0.39 : 1	0.38 : 0.38 : 1	0.70	0.98	0.58
	2.00 : 1.11 : 1	0.51 : 0.56 : 1	0.61	0.99	0.48
	0.70 : 0.11 : 1	0.11 : 0.55 : 1	0.28	0.99	0.21
Fig. 15	2.54 : 0.71 : 1	0.71 : 0.56 : 1	0.82	0.6	0.75
	2.48 : 0.73 : 1	0.73 : 0.38 : 1	0.79	0.35	0.68
	2.06 : 0.49 : 1	0.49 : 0.47 : 1	0.77	0.62	0.65
	2.11 : 0.53 : 1	0.53 : 0.48 : 1	0.68	0.48	0.56
	1.78 : 0.35 : 1	0.35 : 0.44 : 1	0.66	0.65	0.53
	1.24 : 0.28 : 1	0.28 : 0.43 : 1	0.65	0.8	0.54
	0.72 : 0.15 : 1	0.15 : 0.51 : 1	0.42	0.98	0.42

*P_{max} and P_{ave} represent the daily maximum and average PV generation, respectively. D_{max} and D_{ave} are the daily maximum and average electricity demand, respectively.

References

[1] K. Klein, S. Herkel, H.-M. Henning, C. Felsmann, Load shifting using the heating and cooling system of an office building: quantitative potential evaluation for different flexibility and storage options, Appl. Energy 203 (2017) 917–937.
[2] S.Ø. Jensen, A. Marszal-Pomianowska, R. Lollini, W. Pasut, A. Knotzer, P. Engelmann, et al., IEA EBC annex 67 energy flexible buildings, Energy Build. 155 (2017) 25–34.
[3] S. Wang, D-c Gao, R. Tang, F. Xiao, Cooling supply-based HVAC system control for fast demand response of buildings to urgent requests of smart grids, Energy Proc. 103 (2016) 34–39.
[4] J. Sánchez Ramos, M. Pavón Moreno, M. Guerrero Delgado, S. Álvarez Domínguez, F. Cabeza L, Potential of energy flexible buildings: evaluation of DSM strategies using building thermal mass, Energy Build. 203 (2019), 109442.
[5] M. Shakeri, M. Shayestegan, H. Abunima, S.M.S. Reza, M. Akhtaruzzaman, A.R.M. Alamoud, et al., An intelligent system architecture in home energy management systems (HEMS) for efficient demand response in smart grid, Energy Build. 138 (2017) 154–164.
[6] G. Zhao, L. Li, J. Zhang, K.B. Letaief, Residential demand response with power adjustable and unadjustable appliances in smart grid, in: 2013 IEEE International Conference on Communications Workshops (ICC), 2013, pp. 386–390.
[7] H. Zhang, S. Seal, D. Wu, F. Bouffard, B. Boulet, Building energy management with reinforcement learning and model predictive control: a survey, IEEE Access 10 (2022) 27853–27862.
[8] K. Foteinaki, R. Li, T. Péan, C. Rode, J. Salom, Evaluation of energy flexibility of low-energy residential buildings connected to district heating, Energy Build. (2020) 213.
[9] F. Lu, Z. Yu, Y. Zou, X. Yang, Cooling system energy flexibility of a nearly zero-energy office building using building thermal mass: potential evaluation and parametric analysis, Energy Build. (2021) 236.
[10] M. Morari, H. Lee J, Model predictive control: past, present and future, Comput. Chem. Eng. 23 (1999) 667–682.
[11] Y. Ma, F. Borrelli, B. Hencey, A. Packard, S. Bortoff, Model Predictive Control of thermal energy storage in building cooling systems, in: Proceedings of the 48h IEEE Conference on Decision and Control (CDC) Held Jointly with 2009 28th Chinese Control Conference, 2009, pp. 392–397.
[12] I. Hazyuk, C. Ghiaus, D. Penhouet, Optimal temperature control of intermittently heated buildings using Model Predictive Control: Part II – control algorithm, Build. Environ. 51 (2012) 388–394.
[13] S. Prívara, J. Široký, L. Ferkl, J. Cigler, Model predictive control of a building heating system: the first experience, Energy Build. 43 (2011) 564–572.
[14] S. Liu, J. Cao, Y. Wang, W. Chen, Y. Liu, Self-play reinforcement learning with comprehensive critic in computer games, Neurocomputing 449 (2021) 207–213.
[15] R. Zhang, Q. Lv, J. Li, J. Bao, T. Liu, S. Liu, A reinforcement learning method for human-robot collaboration in assembly tasks, Robot. Comput. Integrated Manuf. 73 (2022), 102227.
[16] P. Odonkor, K. Lewis, Automated design of energy efficient control strategies for building clusters using reinforcement learning, J. Mech. Des. (2019) 141.
[17] Z. Jiang, M.J. Risbeck, V. Ramamurti, S. Murugesan, J. Amores, C. Zhang, et al., Building HVAC control with reinforcement learning for reduction of energy cost and demand charge, Energy Build. (2021) 239.
[18] Y. Du, H. Zandi, O. Kotevska, K. Kurte, J. Munk, K. Amasyali, et al., Intelligent multi-zone residential HVAC control strategy based on deep reinforcement learning, Appl. Energy 281 (2021), 116117.
[19] D. Azuatalam, W.-L. Lee, F. de Nijs, A. Liebman, Reinforcement learning for whole-building HVAC control and demand response, Energy and AI 2 (2020).
[20] K. Li, Z. Ma, D. Robinson, W. Lin, Z. Li, A data-driven strategy to forecast next-day electricity usage and peak electricity demand of a building portfolio using cluster analysis, Cubist regression models and Particle Swarm Optimization, J. Clean. Prod. 273 (2020), 123115.
[21] X. Zhou, W. Lin, R. Kumar, P. Cui, Z. Ma, A data-driven strategy using long short term memory models and reinforcement learning to predict building electricity consumption, Appl. Energy 306 (2022), 118078.
[22] M.B. Awan, K. Li, Z. Li, Z. Ma, A data driven performance assessment strategy for centralized chiller systems using data mining techniques and domain knowledge, J. Build. Eng. 41 (2021), 102751.
[23] X. Zhou, W. Lin, P. Cui, Z. Ma, T. Huang, An unsupervised data mining strategy for performance evaluation of ground source heat pump systems, Sustain. Energy Technol. Assessments 46 (2021), 101255.
[24] R.S. Sutton, A.G. Barto, Reinforcement Learning : an Introduction, second ed., The MIT Press, Cambridge, Massachusetts, 2018.
[25] A.T.D. Perera, P. Kamalaruban, Applications of reinforcement learning in energy systems, Renew. Sustain. Energy Rev. 137 (2021), 110618.
[26] T.P. Lillicrap, J.J. Hunt, A. Pritzel, N. Heess, T. Erez, Y. Tassa, et al., Continuous Control with Deep Reinforcement Learning, 2015.
[27] L. Breiman, J.H. Friedman, R.A. Olshen, C.J. Stone, Classification and Regression Trees, Routledge, 2017.
[28] Z. Wang, Y. Wang, R.S. Srinivasan, A novel ensemble learning approach to support building energy use prediction, Energy Build. 159 (2018) 109–122.
[29] AGL business flexible server. https://wwwenergymadeeasygovau/plan?id=AGL238852MBE&postcode=2500, 2022.
[30] A. Jani, H. Karimi, S. Jadid, Hybrid energy management for islanded networked microgrids considering battery energy storage and wasted energy, J. Energy Storage 40 (2021), 102700.
[31] R. Luthander, J. Widén, D. Nilsson, J. Palm, Photovoltaic self-consumption in buildings: a review, Appl. Energy 142 (2015) 80–94.
[32] J. Li, M.A. Danzer, Optimal charge control strategies for stationary photovoltaic battery systems, J. Power Sources 258 (2014) 365–373.
[33] R. Malhotra, A. Sharma, Threshold benchmarking for feature ranking techniques, Bulletin of Electrical Engineering and Informatics 10 (2021) 8 (%J Bulletin of Electrical Engineering and Informatics).